

# Kinetics of polycyclotrimerization of 4,4'-thiodiphenylcyanate

R. H. Lin, J. L. Hong\* and A. C. Su\*

*Institute of Materials Science and Engineering, National Sun Yat-Sen University, Kaohsiung, Taiwan 80424, ROC*

*(Received 21 March 1994; revised 24 October 1994)*

Polycyclotrimerization of 4,4'-thiodiphenylcyanate was studied by means of differential scanning calorimetry. Samples of different impurity levels or different catalyst loadings (*n*-nonylphenol (NP), 1 to 10 phr) were studied. In the absence of added catalyst, the sample with higher impurity level (most likely residual water) underwent polycyclotrimerization at a lower temperature range than the sample of comparatively higher purity, although both samples shared the same apparent activation energy ( $E_a = 93 \text{ kJ mol}^{-1}$ ) and exhibited similar autocatalysed *first-order* characteristics. The lowering of the reaction temperature range was more significant in the presence of NP. Interestingly, kinetic features in this case were quite different from the uncatalysed counterpart: in addition to the expected decrease in the apparent activation energy ( $E_a = 75 \text{ kJ mol}^{-1}$ , independent of the catalyst concentration), the cure reaction followed an autocatalysed *second-order* kinetics. These observations are explained in terms of a mechanistic scheme in which the competition between hydroxyl-catalysed and autocatalytic paths is considered. In particular, formation of NP aggregates  $(\text{NP})_m$ , where  $m \approx 7$  is proposed to account for the less-than-additive catalytic capacity with increasing NP level.

(Keywords: polycyclotrimerization; 4,4'-thiodiphenylcyanate; autocatalysis)

## INTRODUCTION

The polycyclotrimerization of aromatic dicyanates to form a network of *sym*-triazine rings is presumably simple, involving no significant side reactions<sup>1–4</sup>. The reaction leading to the formation of *sym*-triazine rings may be catalysed by transition metal carboxylates or acetylacetonates and by phenols<sup>5–11</sup>. In the absence of externally added catalysts, the polycyclotrimerization reaction is believed to be catalysed by residual hydrogen-donating impurities; no reaction takes place if pure aromatic cyanates are heated<sup>4</sup>. The detailed kinetics of the polycyclotrimerization reaction, however, appears rather complicated as observed from results of kinetic studies in the literature.

Using  $\text{Cr}^{3+}$  acetylacetonate ( $\text{Cr}(\text{acac})_3$ ) as a catalyst, Bonetskaya *et al.*<sup>5,6</sup> studied the polycyclotrimerization of 2,2-bis(4-cyanatophenyl)propane (BCPP) in ditolylmethane by means of infra-red spectroscopy. They observed that there existed a maximum rate (i.e. the reaction bears autocatalytic characteristics) at a definite degree of conversion independent of the initial monomer concentration or the catalyst concentration. This maximum rate itself was proportional to the square-root of catalyst and water concentration and depended linearly on monomer concentration. The relationship between reaction rate and concentration of water suggested the critical role of water as cocatalyst to facilitate the polycyclotrimerization.

The results of this group, however, were not confirmed by other workers. Cure kinetics of a commercialized aromatic dicyanate resin system was studied by Gillham and co-workers<sup>8,12</sup>. For the uncatalysed resin (i.e. without the presence of externally added catalyst), the rate of reaction was slow and could be fitted with the empirical rate expression<sup>12</sup>

$$d\alpha/dt = (k_1 + k_2\alpha)(1 - \alpha)^2 \quad (1)$$

where  $\alpha$  is the fractional conversion and  $k_1$  and  $k_2$  are apparent rate constants. The second term on the right-hand side of equation (1) was due to the consideration of a competing (and presumably autocatalytic) reaction observed in dynamic differential scanning calorimetry (d.s.c.) thermograms as a second exothermic peak<sup>8</sup>. The corresponding activation energies for  $k_1$  and  $k_2$  were 44 and  $134 \text{ kJ mol}^{-1}$ , respectively. In the presence of a mixture of copper naphthenate and *n*-nonylphenol, the rate of polycyclotrimerization was fitted with a simple *n*th-order expression where an optimal value of  $n = 1.872$  was found<sup>8</sup>. Cure behaviour of BCPP in the presence of a mixed catalyst was examined by Osei-Owusu *et al.*<sup>9</sup> An empirical second-order rate expression was established. The rate constant was found to depend linearly on the catalyst concentration.

It may be summarized that results from previous kinetic studies of *sym*-triazine formation do not agree with one another. One apparent reason for this confusion is the difference in the (often complicated) catalyst systems used by different research groups. It is believed that reaction paths of the organometallic catalysts and

\* To whom correspondence should be addressed

the phenolic catalysts (impurity or externally added) can be entirely different: the former proceeds via a coordination/ionic mechanism<sup>5,13</sup> whereas the latter is via a non-ionic, step-growth route<sup>11</sup>. In addition, differences in the reaction medium (solution versus undiluted state) may also have some effects<sup>5,14</sup>.

Reported here are results of our kinetic study for the polycyclotrimerization of 4,4'-thiodiphenylcyanate (TDPC) in bulk by means of d.s.c. Cure kinetics of TDPC without externally added catalyst but with different impurity levels, and that of TDPC with the addition of various amounts of *n*-nonylphenol (NP) as a catalyst, are analysed and discussed.

## EXPERIMENTAL

### Materials

4,4'-Thiodiphenylcyanate was synthesized from 4,4'-thiodiphenol according to the cyanogen bromide method<sup>15</sup>. After removal of the ammonium salt the resulting solution was precipitated with deionized water to obtain a crude product. Two batches of samples were prepared from the crude product. The first batch (denoted as sample A0) was purified twice via recrystallization in carbon tetrachloride; for the second batch (denoted as sample B0), the recrystallization step was performed only once. Sample B0 was therefore considered higher in impurity level. To prepare the externally catalysed samples, different amounts (four levels, ranging from 1 to 10 phr) of NP were added to methyl ethyl ketone solutions of the A0 sample. The solvent was subsequently evaporated under vacuum. These externally catalysed samples were coded as A1, A3, A5 and A10, respectively, according to the amount (in phr) of the added NP.

### Differential scanning calorimetry

Samples approximately 5–8 mg in weight were sealed in hermetic pans and scanned in a differential scanning calorimeter (Perkin–Elmer DSC-7) calibrated by use of an indium standard. The heating rate ( $\phi$ ) was varied from 10 to 40 °C min<sup>-1</sup>, in 10 °C increments. A stream of nitrogen at a flow rate of 20 cm<sup>3</sup> min<sup>-1</sup> was used to purge the d.s.c. cell.

## RESULTS

### As-recrystallized samples

Given in Figure 1 are d.s.c. thermograms of sample A0 at various heating rates. General features of these thermograms include a sharp endothermic peak in the vicinity of 90 °C and a broad exothermic cure peak above 200 °C. The endothermic peak corresponds to melting of the TDPC crystal whereas the exothermic peak corresponds to the polycyclotrimerization reaction. Representative thermograms of samples A0 and B0 at a fixed heating rate are compared in Figure 2. The melting peak in the case of sample B0 is comparatively less sharp, reflecting the relatively impure nature of the sample; more significantly, the cure peak shifted to a lower temperature range, indicating a higher reaction rate.

For the sake of convenience, we assume a relatively simple rate expression of the form

$$d\alpha/dt = kf(\alpha) = Af(\alpha)\exp(-E_a/RT) \quad (2)$$

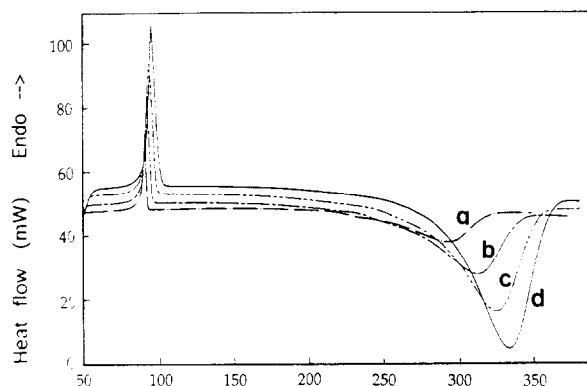


Figure 1 D.s.c. thermograms of sample A0 at various heating rates,  $\phi$  (°C min<sup>-1</sup>): (a) 10; (b) 20; (c) 30; (d) 40

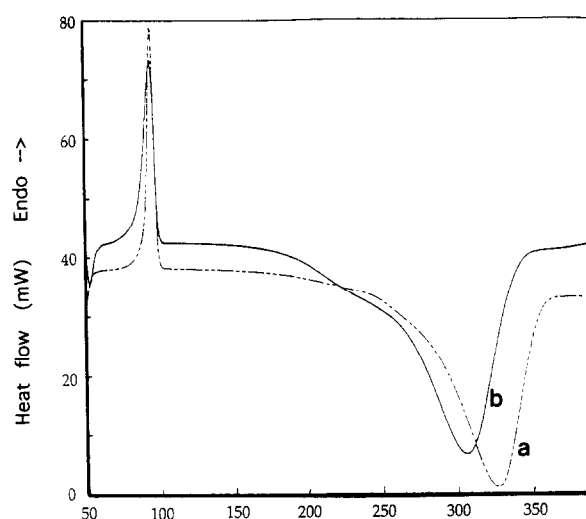


Figure 2 Comparison between d.s.c. thermograms of samples A0 (a) and B0 (b) at a heating rate of 30 °C min<sup>-1</sup>

where  $f(\alpha)$  corresponds to the concentration-dependent part of the rate expression,  $k$  is the rate constant,  $A$  is the pre-exponential factor,  $E_a$  is the apparent activation energy,  $R$  is the gas constant and  $T$  is the absolute temperature. The value of  $E_a$  may be estimated from the heating rate dependence of the peak temperature ( $T_p$ ) of the cure exotherm according to<sup>16</sup>

$$E_a = -0.951R \, d \ln \phi / d(1/T_p) \quad (3)$$

Linear regression analyses of the experimental  $\phi$ – $T_p$  data have yielded a common value of  $E_a = 92.6 \pm 0.3$  kJ mol<sup>-1</sup> for the two samples. We may then proceed to obtain  $Af(\alpha)$  from the experimental  $d\alpha/dt$  data using

$$Af(\alpha) = [d\alpha/dt] \exp(E_a/RT) \quad (4)$$

The plot of  $Af(\alpha)/(1-\alpha)$  against  $\alpha$  for sample A0 is given in Figure 3, where a routine linear regression yields

$$Af(\alpha) = 0.72 \times 10^8 (1.52 + \alpha)(1 - \alpha) \text{ min}^{-1} \quad (5)$$

A parallel analysis for sample B0 yields

$$Af(\alpha) = 1.67 \times 10^8 (1.52 + \alpha)(1 - \alpha) \text{ min}^{-1} \quad (6)$$

Calculated conversion curves using equations (2) and (5) or (6) are compared with the experimental counterparts in Figure 4. As may be observed, the experimental results

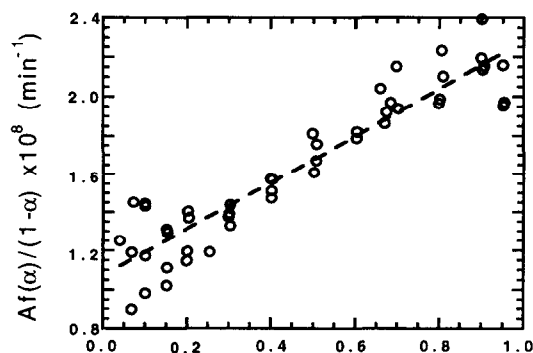


**Figure 3** Plot of  $Af(\alpha)/(1-\alpha)$  versus  $\alpha$  for sample A0. Symbols represent data from dynamic d.s.c. scans at different heating rates; dashed line is the least-squares fit

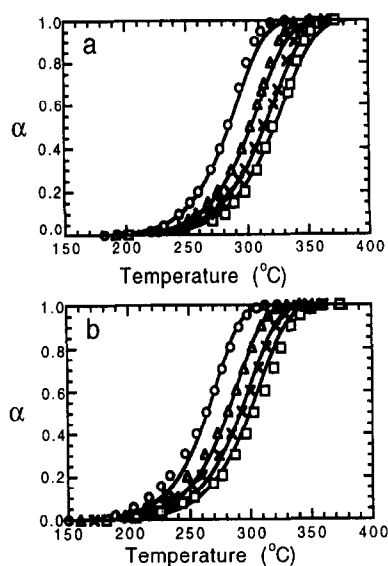


**Figure 4** Comparison between experimentally determined conversion curves (symbols) and those (solid lines) calculated from the empirical rate expressions (i.e. equations (2) and (7)): (a) sample A0; (b) sample B0. Corresponding heating rates of the conversion curves are, from left to right, 10, 20, 30 and 40°C min<sup>-1</sup>, respectively

are reasonably well represented by these empirical expressions.

#### Externally catalysed samples

Representative d.s.c. thermograms of the NP-catalysed samples are given in Figure 5. At a fixed heating rate, the cure peak shifts to lower temperatures with increasing NP concentration. The kinetic analysis procedure described in the preceding paragraph was repeated for each level of catalyst loading. The apparent activation energy was found to be  $75.2 \pm 1.1$  kJ mol<sup>-1</sup> for the four catalyst levels used. However, a slight modification in the concentration-dependent part of the rate expression had to be made. The autocatalysed first-order rate expression in equations (5) and (6), i.e.

$$d\alpha/dt = H(b + \alpha)(1 - \alpha) \exp(-E_a/RT) \quad (7)$$

was found unable to give proper fit to experimental data. Alternatively, an autocatalysed *second-order* equation

$$d\alpha/dt = H(b + \alpha)(1 - \alpha)^2 \exp(-E_a/RT) \quad (8)$$

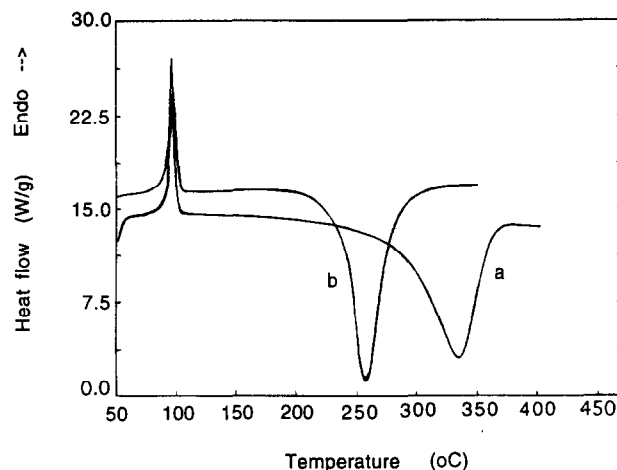


**Figure 5** Comparison between d.s.c. thermograms of samples A0 (a) and A1 (b) at a heating rate of 30°C min<sup>-1</sup>

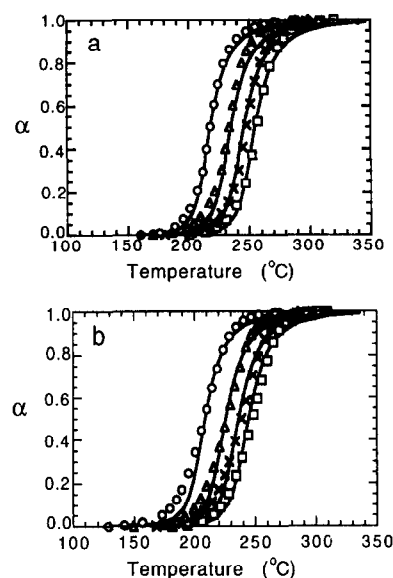


**Figure 6** Comparison between experimentally determined conversion curves (symbols) and those (solid lines) calculated from the empirical rate expressions (i.e. equations (2) and (8)): (a) sample A1; (b) sample A10. Corresponding heating rates of the conversion curves are, from left to right, 10, 20, 30 and 40°C min<sup>-1</sup>, respectively

was more satisfactory in representing experimental results, as shown in Figure 6. Values of the kinetic parameters in equations (7) or (8) for all samples are summarized in Table 1. The value of  $H$  in NP-catalysed reaction increases with the level of catalyst loading, but a closer look indicates that the catalytic capacity does not increase in proportion with the amount of added NP.

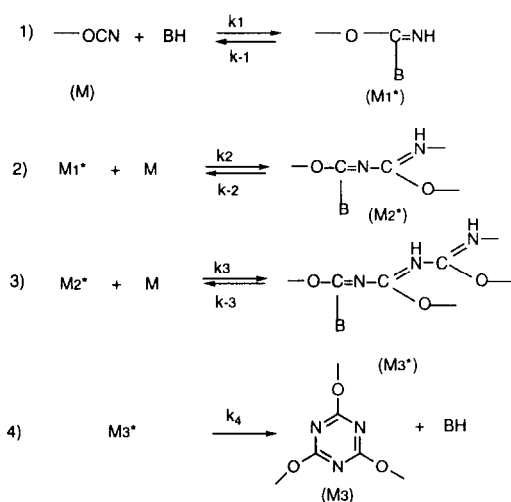
#### DISCUSSION

The fact that rate expressions of the as-recrystallized and the externally catalysed samples can be arranged into the common forms of equations (7) and (8), respectively, implies an important kinetic feature in the polycyclotrimerization of the present system. The parameter  $H$  may be taken as representing the amount of impurity (and therefore the catalytic capacity) for as-recrystallized samples or the catalyst concentration for externally

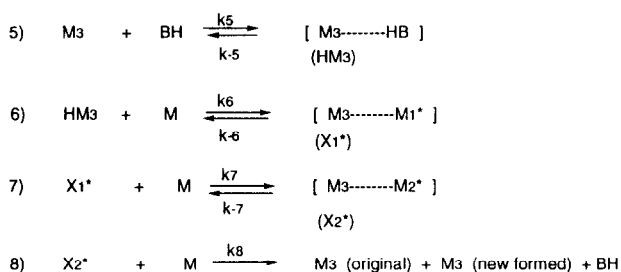
**Table 1** Values of kinetic parameters (cf. equations (7) and (8)) for as-recrystallized and externally catalysed 4,4'-thiodiphenylcyanate

Sample code	Amount of externally added catalyst, $C_0$ (phr)	$H \times 10^{-8}$ ( $\text{min}^{-1}$ )
As-recrystallized samples		
(Equation (7), $b = 1.52$ , $E_a = 92.6 \text{ kJ mol}^{-1}$ )		
A0	—	0.72
B0	—	1.67
air-exposed	—	2.50
n-Nonylphenol-catalysed samples		
(Equation (8), $b = 0.008$ , $E_a = 75.2 \text{ kJ mol}^{-1}$ )		
A1	1.0	2.60
A3	3.0	2.95
A5	4.9	3.15
A10	10	3.65

a) Hydroxyl-catalyzed reaction



b) Autocatalytic reaction



**Scheme 1** Proposed mechanistic paths for polycyclotrimerization of 4,4'-thiodiphenylcyanate

catalysed samples relative to the autoacceleration effect from the *sym*-triazine product<sup>7,11</sup>. This interpretation is in accordance with the qualitative picture previously reported for the polycyclotrimerization of aromatic cyanates. The lower value of  $E_a$  may reasonably be expected for the externally catalysed case. The change in the reaction order is somewhat unexpected but can be readily explained in terms of the mechanism proposed in *Scheme 1*.

Scheme 1 contains both of the hydroxyl-catalysed and the autocatalytic paths. Mechanistic steps in the hydroxyl-catalysed path are basically similar to those proposed by Baucr *et al.*<sup>11</sup> except that all intermediate species (such as  $HM_3$ ,  $X_1^*$ ,  $X_2^*$ ) involved in the autocatalysed part are assumed to be hydrogen-bonded to the

electron-donating nitrogen atoms of the *sym*-triazine ring. Steps in the autocatalytic part are assumed to run in a parallel manner with those in the hydroxyl-catalysed part. Under the assumption of pseudo-steady state and that steps 1 and 6 are the rate-determining steps, a routine kinetic analysis on this mechanistic scheme results in a kinetic expression of

$$-d[\mathbf{M}]/dt = [\mathbf{BH}][\mathbf{M}]\{k_1 + (k_5/k_{-5})k_6[\mathbf{M}_3]\} \quad (9)$$

where  $k_1$  and  $k_6$  are rate constants of the respective forward reactions of steps 1 and 6, and  $[M]$ ,  $[BH]$  and  $[M_3]$  represent concentrations of the monomer, the catalyst and the *sym*-triazine moiety, respectively. This first-order autocatalytic rate expression is consistent with our experimental findings for ‘uncatalysed’ TDPC. Kinetic analysis with the same pseudo-steady state assumption but taking steps 2 and 7 as rate-determining steps results in a form

$$-d[\mathbf{M}]/dt = [\mathbf{BH}][\mathbf{M}]^2 \{ (k_1 k_2 / k_{-1}) + K(k_6 / k_{-6}) k_7 [\mathbf{M}_3] \} \quad (10)$$

where  $K$  is the equilibrium constant of step 5 and  $k_1$ ,  $k_2$ ,  $k_6$ ,  $k_7$  and  $k_{-1}$  are rate constants of the respective forward and backward reactions. This coincides with our experimental observations for NP-catalysed series.

Bauer *et al.*<sup>11</sup> previously suggested that residual phenols (due to incomplete conversion to cyanate) are the species responsible for the initiation of polycyclotrimerization of 'uncatalysed' dicyanates synthesized via the cyanogen bromide route; however, the observed differences in the reaction order and the relative weighting of autocatalytic terms between uncatalysed and externally catalysed reactions here cannot be explained if phenols were the main species involved in both cases. Instead, we suggest that the main catalyst (BH) involved here in the uncatalysed polycyclotrimerization is the residual water, the species formerly proposed to be an active component in Cr(acac)<sub>3</sub>-catalysed reaction of 2,2-bis(4,4'-dicyanatophenyl) propane.<sup>5,6</sup> In other words, steps 1 and 6 are the controlling steps in the 'uncatalysed' reactions due to the relative weak acidity of H<sub>2</sub>O and the necessity of proton transfer in these reaction steps. In contrast, the addition of NP, a stronger acid, to cyanates in the externally catalysed reaction makes proton transfer relatively easy, shifting the controlling steps to steps 2 and 7.

To verify the assumed role of residual water in the 'uncatalysed' samples, sample B0 was intentionally exposed to ambient air for two days and the d.s.c. analysis was then repeated. A lowering of the reaction temperature range compared with the as-recrystallized B0 is evident in *Figure 7*. This suggests that the absorbed moisture may indeed function as a catalyst. Dynamic d.s.c. scans of the air-exposed B0 at heating rates of 10, 20 and 30°C min<sup>-1</sup> resulted in an apparent activation energy value of 92.4 kJ mol<sup>-1</sup>, in excellent agreement with that (92.6 kJ mol<sup>-1</sup>) for A0 and B0. A rate expression of  $Af(\alpha) = 2.50 \times 10^8 (1.52 + \alpha)(1 - \alpha) \text{ min}^{-1}$  is assigned to this air-exposed B0 sample. The higher *H* value (cf. equations (5) and (6)) is also consistent with the higher residual water content in this sample.

It may be noted that the value of  $H$  is not in proportion with NP content and does not appear to diminish to zero with decreasing NP level. This may be

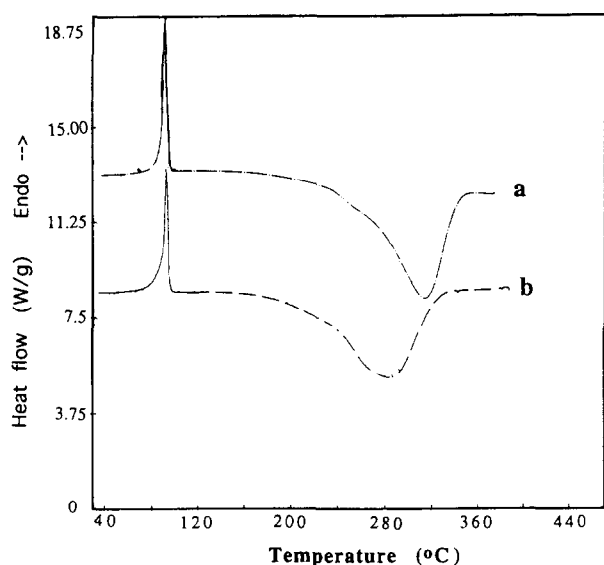


Figure 7 Comparison between d.s.c. thermograms of as-recrystallized sample B0 (a) and air-exposed B0 (b) at a heating rate of  $20^{\circ}\text{C min}^{-1}$

attributed to the formation of NP aggregates (or micelles),  $(\text{NP})_m$ , via intermolecular hydrogen bonding. With the inherent hydrophobic *n*-nonylphenyl and hydrophilic hydroxyl moieties in NP, formation of micelle structure is a distinct possibility. This is supported by the reported use of NP as an emulsifier in oil industries<sup>17</sup>. If it is assumed that only free NP can act effectively as catalyst, the equilibrium between NP and  $(\text{NP})_m$  dictates that the relationship between  $H$  (effective NP concentration) and  $C_0$  (total amount of added NP) should follow

$$\ln H = m^{-1} \ln C_0 + \text{constant} \quad (11)$$

where  $m$  is the aggregation number. Logarithmic plot of  $H$  versus  $C_0$  in Figure 8 resulted in a straight line with slope  $m^{-1} = 0.144$  (i.e.  $m \approx 7$ ). It is then gratifying to observe that the plot of  $H$  versus  $C_0^{1/7}$  in Figure 9 yields a straight line passing through the origin.

## CONCLUSIONS

Kinetics of polycyclotrimerization of 4,4'-thiodiphenylcyanate was studied by means of differential scanning calorimetry. In the absence of added catalyst, the polycyclotrimerization reactions of samples A0 and B0 shared the same apparent activation energy ( $E_a \approx 93 \text{ kJ mol}^{-1}$ ) and followed an autocatalysed first-order rate expression. Polycyclotrimerizations in the presence of an externally added catalyst (*n*-nonylphenol, NP) proceeded at lower temperatures compared with the uncatalysed case. In addition to the expected decrease of activation energy ( $E_a \approx 75 \text{ kJ mol}^{-1}$ , independent of the catalyst concentration), the cure reaction exhibited an autocatalysed second-order kinetics. Details of the kinetic features were discussed in terms of mechanistic paths. In particular, residual water is considered as the active species in the 'uncatalysed' samples. In the presence of NP, formation of  $(\text{NP})_m$  aggregates is proposed to explain the non-additive catalytic capacity with increasing NP level.

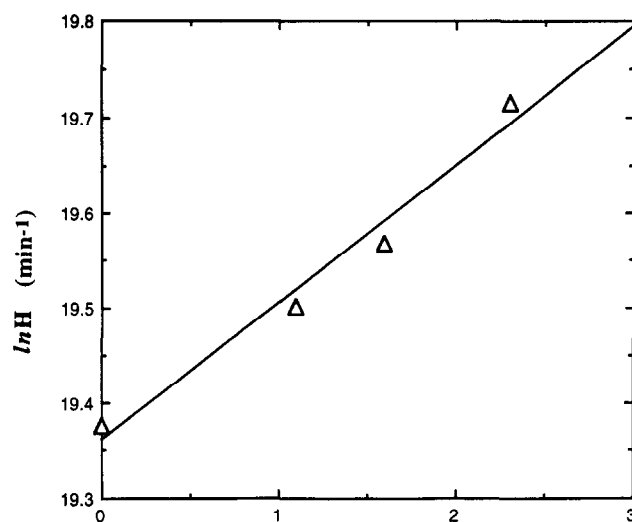


Figure 8 Logarithmic relationship between  $H$  (cf. equation (11)) and the amount of added *n*-nonylphenol ( $C_0$ )

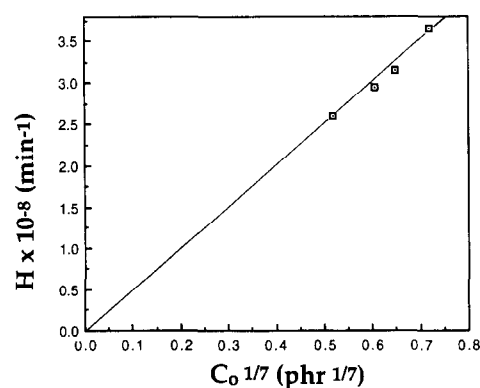


Figure 9 Plot of  $H$  versus  $C_0^{1/7}$

## ACKNOWLEDGEMENTS

This work was financially supported by the National Science Council, ROC, under contract number NSC82-0405-E110-030. Thanks are also extended to the National Kaohsiung Institute of Technology and the Ministry of Education, ROC, for the support endowed to R.H.L. in the form of leave-with-pay.

## REFERENCES

- 1 Ayano, S. *Chem. Economy Eng. Rev.* 1978, **10**(3), 25
- 2 Wertz, D. H. and Prevorsek, D. C. *Polym. Eng. Sci.* 1985, **25**, 804
- 3 Penczek, P. and Kaminska, W. *Adv. Polym. Sci.* 1990, **97**, 41
- 4 Bauer, M. *M.S. Thesis*, Academy of Sciences of the GRD, Berlin, 1980
- 5 Bonetskaya, A. K., Kravchenko, M. A., Frenkel, Ts. M., Pankratov, V. A., Vinogradova, S. V. and Korshak, V. V. *Polym. Sci. USSR* 1977, **19**, 1201
- 6 Bonetskaya, A. K., Ivanov, V. V., Kravchenko, M. A., Pankratov, V. A., Frenkel, Ts. M., Korshak, V. V. and Vinogradova, S. V. *Polym. Sci. USSR* 1980, **22**, 845
- 7 Shimp, D. A. *Polym. Mater. Sci. Eng.* 1986, **54**, 107
- 8 Simon, S. L., Gillham, J. K. and Shimp, D. A. *Polym. Mater. Sci. Eng.* 1990, **62**, 96
- 9 Osei-Owusu, A., Martin, G. C. and Gotro, J. T. *Polym. Eng. Sci.* 1992, **32**, 535

- 10 Bauer, M., Bauer, J. and Garske, B. *Acta Polymerica* 1986, **37**, 604
- 11 Bauer, M., Bauer, J. and Kuhn, G. *Acta Polymerica* 1986, **37**, 715
- 12 Simon, S. L. and Gillham, J. K. *Polym. Prepr.* 1991, **32**(2), 182
- 13 Korshak, V. V., Pankratov, V. A., Ladovskaya, A. A. and Vonogradova, S. V. *J. Polym. Sci., Polym. Chem.* 1978, **16**, 1697
- 14 Fyfe, C. A., Niu, J., Rettig, S. J., Burlingson, N. E., Reidsema, C. M., Wang, D. W. and Poliks, M. *Macromolecules* 1992, **25**, 6289
- 15 Grigat, E. and Putters, R. *Chem. Ber.* 1964, **97**, 3013
- 16 Prime, R. B. in 'Thermal Characterization of Polymeric Materials' (Ed. E. A. Turi), Academic Press, New York, 1981, ch. 5
- 17 *Chem. Abstr.* 1976, **84**, 92451h